The Spectral Energy Distribution of Galaxies
Proceedings IAU Symposium No. 284, 2011
R.J. Tuffs & C.C. Popescu, eds.

doi:10.1017/S1743921312009416

AKARI/IRC broadband mid-infrared data as an indicator of the Star Formation Rate

Fang-Ting Yuan[1], Tsutomu T. Takeuchi[1], Véronique Buat[2], Sébastien Heinis[2], Elodie Giovannoli[2], Katsuhiro L. Murata[1], Jorge Iglesias-Páramo[3,4] and Denis Burgarella[2]

[1]Division of Particle and Astrophysical Sciences,
Nagoya University, JAPAN
email: `yuan.fangting, takeuchi.tsutomu, murata.katsuhiro@g.mbox.nagoya-u.ac.jp`

[2]Laboratoire d'Astrophysique de Marseille, OAMP,
Université Aix-Marseille, FRANCE
email: `veronique.buat, sebastien.heinis, elodie.giovannoli, denis.burgarella@oamp.fr`

[3]Instituto de Astrofísica de Andalucía (IAA - CSIC),
Glorieta de la Astronomía s.n., SPAIN

[4]Centro Astronómico Hispano Alemán, SPAIN
email: jiglesia@iaa.es

Abstract. With the goal of constructing Star-Formation Rates (SFR) from AKARI Infrared Camera (IRC) data, we analyzed an IR-selected GALEX-SDSS-2MASS-AKARI(IRC & Far-Infrared Surveyor) sample of 153 nearby galaxies. The far-infrared fluxes were obtained from AKARI diffuse maps to correct the underestimation for extended sources raised by PSF photometry. SFRs of these galaxies were derived using the SED fitting program CIGALE. In spite of complicated features contained in these bands, both the *S9W* and *L18W* emissions correlate with the SFR of galaxies. The SFR calibrations using *S9W* and *L18W* are presented for the first time. These calibrations agree well with previous work based on Spitzer data within the scatter, and should be applicable to dust-rich galaxies.

Keywords. infrared: galaxies, ISM: dust, extinction, stars: formation

1. Introduction

Measurements of star formation activity are fundamental to studies of the formation and evolution of galaxies. Numerous efforts have been made to find reliable and convenient star formation rate (SFR) indicators. Apart from the most frequently used indicators, such as FUV continuum, optical recombination lines and FIR continuum (Kennicutt 1998), the mid-infrared (MIR) monochromatic fluxes have also been investigated as SFR indicators. The MIR emission is contributed by several components, including the polycyclic aromatic hydrocarbon (PAH) features, the continuum from stochastically-heated very small grains, silicate absorption at 9.7 and 18 μm, molecular hydrogen lines and fine-structure lines (Leger & Puget 1984; Desert *et al.* 1990; Draine & Li 2007; Treyer *et al.* 2010). the MIR-SFR relation was intensively studied using Spitzer IRAC 8 μm and MIPS 24 μm photometry data and spectral data (e.g., Calzetti *et al.* 2007; Kennicutt *et al.* 2009; Rieke *et al.* 2009). Nevertheless, there is still a debate about the reliability of MIR indicators because of the complicated features it contains.

The recently released AKARI/IRC Point Source Catalogue Version β-1 (hereafter IRCPSC) provides positions and fluxes of sources detected in the all-sky survey in the *S9W* (9 μm) and *L18W* (18 μm) bands (Ishihara *et al.* 2010). Because of the copious amounts

Table 1. Brief summary of the sample.

Survey	Band	Wavelength (μm)	Nb. of sources
GALEX	FUV, NUV	0.153, 0.231	153
SDSS	u, g, r, i, z	0.355, 0.469, 0.617, 0.748, 0.893	153
2MASS	J, H, Ks	1.244, 1.655, 2.169	153
IRAS*	band-1, 2, 3, 4	12, 25, 60, 100	153
AKARI IRC	*S9W*	9	126
AKARI IRC	*L18W*	18	106
AKARI FIS	*N60*, *Wide-S*, *Wide-L*, *N160**	65, 90, 140, 160	153

* Data were not used for SED fitting.

of MIR data, it would be useful if there is a benchmark of SFR measurement. Compared with the Spitzer 8 and 24 μm bands, the AKARI IRC *S9W* and *L18W* bands cover a wider wavelength range, including silicate absorption features in both bands and emission contributed by large PAH molecules in the *L18W* band. This work is done to investigate whether and to what degree AKARI broadband MIR data could trace SFRs, and how the inclusion of silicate absorption and longer wavelength PAH feature affects the results.

2. Data and Method

We cross-identified IRCPSC with the multi-wavelength data constructed by Takeuchi *et al.* 2010. The original sample is based on a selection using the IRAS-PSC*z* Saunders *et al.* 2000 and AKARI/FIS Bright Source Catalogue (hereafter FISBSC) data (I. Yamamura *et al.* 2008). These galaxies are then cross-matched to sources detected by GALEX, 2MASS and SDSS. The FISBSC flux density for extended sources would no longer be accurate because of the point source extraction procedure. This is confirmed by a comparison with similar bands in IRAS co-added fluxes, which are specially calculated for extended sources (Saunders *et al.* 2000). Therefore, the fluxes for extended sources are replaced by Äutofluxes derived from AKARI diffuse maps using Source Extractor. The data used in the present study are summarized in Table 1.

The SED fitting program CIGALE (Noll *et al.* 2009) is used to calculate the SFR for our sample. CIGALE was developed to derive highly reliable galaxy properties by fitting the UV/optical SEDs and the related dust emission at the same time, i.e., the stellar population synthesized models are connected with infrared templates by the balance of the energy of dust emission and absorption. A detailed description of CIGALE could be found in Noll *et al.* (2009), Buat *et al.* (2010) and Giovannoli *et al.* (2010) - see also Buat *et al.* (this volume).

3. Result and Conclusion

Regression analysis was conducted to investigate the MIR-SFR relations. SFRs converted from AKARI MIR fluxes were compared with the ones from Spitzer MIR fluxes to test the reliability of AKARI MIR-SFR calibrations. We summarize our results and conclusions as follows:

(a) Both 9 μm and 18 μm luminosities correlate with SFRs and thus could be converted into SFRs (Fig. 1). The correlation equations are given by

$$\log \frac{\mathrm{SFR}}{M_\odot/\mathrm{yr}} = (0.99 \pm 0.03) \log \frac{L_9}{L_\odot} - (9.02 \pm 0.32) \tag{3.1}$$

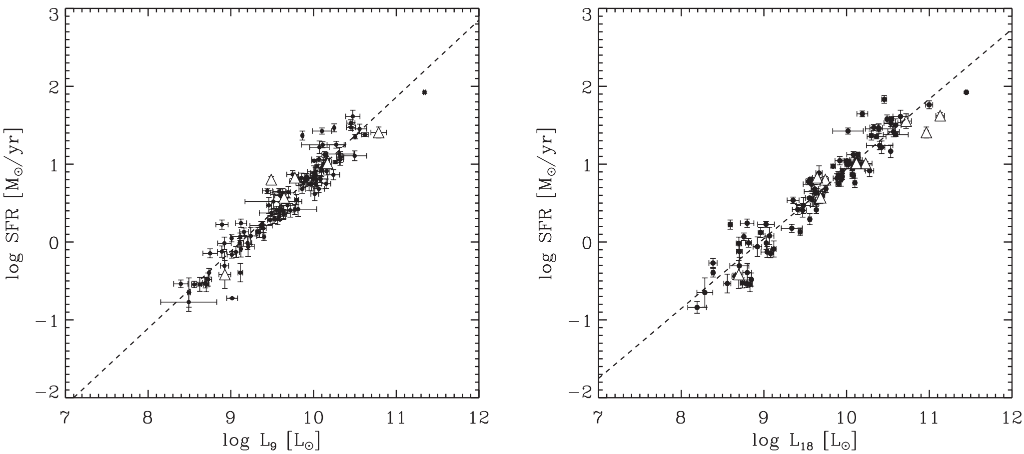

Figure 1. The MIR-SFR relation. The dashed line shows the fitting result. The triangles denote AGNs.

$$\log \frac{\mathrm{SFR}}{M_\odot/\mathrm{yr}} = (0.90 \pm 0.03) \log \frac{L_{18}}{L_\odot} - (8.03 \pm 0.30). \tag{3.2}$$

The scatters are 0.18 and 0.20 for 9 and 18 μm, respectively.

(*b*) A combination of FUV and MIR luminosities barely reduces the scatters (0.17 and 0.20 dex for 9 and 18 μm, respectively), indicating that unobscured UV photons are not the only reason for variations in the MIR-SFR relation.

(*c*) The comparison of the SFRs derived from Equations 3.1 and 3.2 with the ones derived from Spitzer MIR-SFR relations shows that the silicate absorption included in *S9W* (9 μm) and *L18W* (18 μm) bands little affects the results. The discrepancies, if any, are well within the uncertainties.

(*d*) AGNs in the sample show no discrepancy with normal galaxies in the MIR-SFR diagrams. However, AGNs do show lower MIR values than normal galaxies on average, which probably indicates that small PAH molecules are destructed by the harsh radiation from AGNs.

References

Buat, V., *et al.* 2010, *A&A*, in press

Calzetti, D., *et al.* 2007, *ApJ*, 666, 870

Desert, F.-X., Boulanger, F., & Puget, J. L. 1990, *A&A*, 237, 215

Draine, B. T. & Li, A. 2007, *ApJ*, 657, 810

Giovannoli, E., Buat, V., Noll, S., Burgarella, D., & Magnelli, B. 2011, *A&A*, 525, A150

Ishihara, D., *et al.* 2010, *A&A*, 514, A1

Kennicutt, R. C., Jr. 1998, *ARAA*, 36, 189

Kennicutt, R. C., *et al.* 2009, *ApJ*, 703, 1672

Leger, A. & Puget, J. L. 1984, *A&A*, 137, L5

Noll, S., Burgarella, D., Giovannoli, E., Buat, V., Marcillac, D., & Muñoz-Mateos, J. C. 2009, *A&A*, 507, 1793

Rieke, G. H., Alonso-Herrero, A., Weiner, B. J., Pérez-González, P. G., Blaylock, M., Donley, J. L., & Marcillac, D. 2009, *ApJ*, 692, 556

Saunders, W., *et al.* 2000, *MNRAS*, 317, 55

Takeuchi, T. T., *et al.* 2010, *A&A*, 514, A4

Treyer, M., *et al.* 2010, *ApJ*, 719, 1191

Yamamura, I., Fukuda, Y., & Makiuti, S. 2008, AKARI/FIS all-sky Survey Bright Source Catalogue Version β-1 Release Note (Rev. 1)